

1 We thank the reviewers for finding our problem relevant (R4), the game-theoretic formulation of adversarial attacks and  
 2 defenses novel (R1, R3, R4) and the paper clearly written (R1, R2, R3, R4). The main critique is that the assumptions  
 3 (local-linearity, restrictions on defender strategies) are strong. However, the reviewers did not point to prior work that is  
 4 able to handle our setting. We believe our solution under these assumptions is a necessary stepping stone which lays the  
 5 foundations for future theoretical advancements into additive attacks and defenses. We now provide detailed responses:

6 **[R1, R2, R3, R4] Validity of locally-linear assumption.** While the as-  
 7 sumption of local-linearity might seem strong at first, there is ample empiri-  
 8 cal evidence of its validity for neural networks. Fig. A shows the decision  
 9 boundaries of a CNN trained on CIFAR-10 in a  $\epsilon$  neighbourhood of many  
 10 randomly-selected images, where white denotes the predicted class and  
 11 other shades denote other classes. It can be seen that, locally, the boundary  
 12 is approximately linear. This *linearity hypothesis* was proposed in [C1] and  
 13 further explored in [C2] (showing empirical evidence) and [24] (linking  
 14 to the existence of universal adversarial perturbations). Recent studies  
 15 [C3], [C4] improve Deep Neural Networks’ robustness by promoting local-  
 16 linearity. Hence, we stress that our work *does* partially apply to modern  
 17 real-world classifiers, and is certainly not limited to linear classifiers. [C1]:  
 18 Goodfellow et. al. Explaining and harnessing adversarial examples. [C2]:  
 19 Warde-Farley et. al. Adversarial Perturbations of Deep Neural Networks.  
 20 [C3]: Lee et. al. Towards Robust, Locally Linear Deep Networks. [C4]:  
 21 Qin et. al. Adversarial Robustness through Local Linearization.

22 **[R1, R2] Do images typically lie near non-linear parts of the decision  
 23 boundary?** Yes, empirical evidence on real world networks as in Fig. A  
 24 suggests that we almost never find a decision-boundary corner in a  $2\epsilon$  neigh-  
 25 bourhood around the image. However, these networks partition the input  
 26 space into thousands of polyhedra, and the problem of efficiently verifying  
 27 whether a given input image lies in a linear-region far from any vertices or  
 28 edges of these polyhedra is an open research question [C3].

29 **[R1] Strong assumption on defender’s knowledge.** The design of a game  
 30 theoretic framework for analyzing attacks and defenses in a level playing field requires imposing constraints that prevent  
 31 the attacker or the defender from always winning. We thus intentionally do not work in a situation where the classifier  
 32 is publicly released for attack. Instead, we want to model the reality that the defender will train the classifier knowing  
 33 the possible attacks, and in turn the attacker will create new attacks knowing that the publisher was aware of possible  
 34 attacks, and so on. This precisely leads to the game-theoretic notion of *perfect knowledge* that we use in Section 2.

35 **[R3, R4] Strong assumptions on defender’s strategies.** As pointed out by R4, obtaining the optimal defense in our  
 36 current robust set is already a hard problem. Extending the set to include perturbations dependent on the data-point  $x$  will  
 37 lead to more complex robust sets, and this is a direction for future work. A first step could be to let  $\mathcal{A}_d$  contain all linear  
 38 transformations projected to the set of allowed perturbations i.e.  $\mathcal{A}_d = \{f_M | f_M : \mathcal{X} \rightarrow \mathcal{Y} \text{ s.t. } f_M(x) = \Pi_{\mathcal{Y}}(Mx)\}$ .

39 **[R3, R4] Scalability of the optimization procedure.** As R4 correctly notes, the optimization problem (7) is hard,  
 40 and we present an approximate solution which currently works for small datasets as shown in Table A (it takes  $< 10$   
 41 seconds for MNIST, FMNIST). In ongoing work, we are scaling it to larger datasets by exploiting the fact that (7) is a  
 42 convex-maximization problem and applying techniques from the classical literature on efficient approximations to (7).

43 **[R2] Extensions to multiple classes, non-ReLU activations, incorpo-  
 44 rating test accuracy.** We thank R2 for the suggestions. They are excellent  
 45 directions for future work. We will add [Sengupta et. al.] to prior work.

46 **[R2, R3] Experiments on other datasets.** In our experiments we used  
 47  $\epsilon = 4$ . Table A shows the result of repeating our experiment in Table 1  
 48 of the paper (the column Approximate Accuracy is shown) over all the  
 49 55 pairs of classes in MNIST and FMNIST. It can be seen that the trends  
 50 observed in the paper hold even when the experiment is repeated over  
 51 multiple pairs.

52 **[R2, R3] Minor writing issues** We will fix the typos in Eq. (33), CW method reference, and clarify that we are not  
 53 using an isotropic Gaussian for randomized smoothing.

54 **[R2] Is PGD better than FGM against our defense?** No. Under the locally linear assumption, FGM performs better  
 55 than PGD (Table 1:  $48.3 < 85.6$  and  $94.5 < 99.1$ ) as expected by Lemma 2. The same trend is seen in Table A.

56 **[R4] Is there a PAC style argument?** Yes, Sec. 5 establishes a PAC-style bound: The estimated solution is  $v_n^*$ ,  
 57 and the optimal one is  $v^*$ . Eq. (16)-(18) upper bound the difference between the objectives by a quantity  $\alpha$ , i.e.  
 58  $\phi(v^*) - \phi(v_n^*) \leq \alpha$ . Eq. (19) establishes that the expectation of  $\alpha$  is upper-bounded by a small quantity  $\beta$ , i.e.  
 59  $\mathbb{E}[\alpha] \leq \beta$ . Using  $\alpha$  in Eq. (10) now yields  $\Pr[\phi(v^*) - \phi(v_n^*) - \beta > \epsilon] \leq \exp(-2n\epsilon^2)$ , which is a PAC bound.

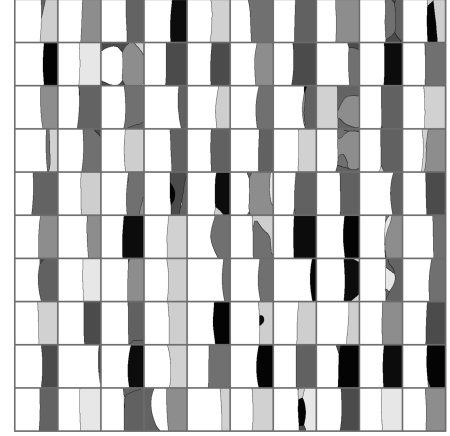


Figure A: Church-Window plots for a CNN  $f$  reproduced from Fig. 11.2 of [C2]. Each plot shows  $f(x + au + bv)$  for  $a, b \in [-\epsilon, \epsilon]$ , where  $\mathbf{u}$  is the FGM direction,  $\mathbf{v}$  is a random direction orthogonal to  $\mathbf{u}$  and  $\mathbf{x}$  is a random data-point from CIFAR-10. White denotes the class  $f(\mathbf{x})$ , and other shades denote other classes.

Table A: Mean (Variance) over  $\binom{10}{2}$  pairs.

| Attack | Defense | MNIST (%)   | FMNIST (%) |
|--------|---------|-------------|------------|
| -      | -       | 99.9 (0.0)  | 99.9 (0.1) |
| FGM    | -       | 53.3 (10.0) | 47.4 (5.1) |
| FGM    | SMOOTH  | 71.2 (14.2) | 67.4 (9.0) |
| PGD    | -       | 71.9 (12.0) | 74.7 (7.3) |
| PGD    | SMOOTH  | 94.0 (4.0)  | 90.3 (8.5) |